Published in final edited form as:
Mol Neurobiol. 2015 February ; 51(1): 43–56. doi:10.1007/s12035-014-8691-z.

Catalytic Immunoglobulin Gene Delivery in a Mouse Model of Alzheimer's Disease: Prophylactic and Therapeutic Applications

Jinghong Kou[1], **Junling Yang**[1], **Jeong-Eun Lim**[1], **Abhinandan Pattanayak**[1], **Min Song**[1], **Stephanie Planque**[2], **Sudhir Paul**[2], and **Ken-ichiro Fukuchi**[1,*]

[1]Department of Cancer Biology and Pharmacology, University of Illinois College of Medicine at Peoria, Peoria, Illinois 61656, USA

[2]Chemical Immunology Research Center, Department of Pathology and Laboratory Medicine, University of Texas Houston Medical School, Houston, Texas 77030, USA

Abstract

Accumulation of amyloid beta-peptide (Aβ) in the brain is hypothesized to be a causal event leading to dementia in Alzheimer's disease (AD). Aβ vaccination removes Aβ deposits from the brain. Aβ immunotherapy, however, may cause T cell- and/or Fc-receptor-mediated brain inflammation and relocate parenchymal Aβ deposits to blood vessels leading to cerebral hemorrhages. Because catalytic antibodies do not form stable immune complexes and Aβ fragments produced by catalytic antibodies are less likely to form aggregates, Aβ-specific catalytic antibodies may have safer therapeutic profiles than reversibly-binding anti-Aβ antibodies. Additionally, catalytic antibodies may remove Aβ more efficiently than binding antibodies because a single catalytic antibody can hydrolyze thousands of Aβ molecules. We previously isolated Aβ-specific catalytic antibody, IgV_L5D3, with strong Aβ-hydrolyzing activity. Here, we evaluated the prophylactic and therapeutic efficacy of brain-targeted IgV_L5D3 gene delivery via recombinant adeno-associated virus serotype 9 (rAAV9) in an AD mouse model. One single injection of rAAV9-IgV_L5D3 into the right ventricle of AD model mice yielded widespread, high expression of IgV_L5D3 in the unilateral hemisphere. IgV_L5D3 expression was readily detectable in the contralateral hemisphere but to a much lesser extent. IgV_L5D3 expression was also confirmed in the cerebrospinal fluid. Prophylactic and therapeutic injection of rAAV9-IgV_L5D3 reduced Aβ load in the ipsilateral hippocampus of AD model mice. No evidence of hemorrhages, increased vascular amyloid deposits, increased pro-inflammatory cytokines or infiltrating T cells in the brains was found in the experimental animals. AAV9-mediated anti-Aβ catalytic antibody brain delivery can be prophylactic and therapeutic options for AD.

Keywords

Alzheimer's disease; amyloid; inflammation; antibody; adeno-associated virus; immunotherapy

*Corresponding author: kfukuchi@uic.edu; T - 309-671-8545; F - 309-671-8403.

Competing Interests
The authors declare that they have no conflict of interest.

Introduction

One of the cardinal pathological changes in Alzheimer's disease (AD) is the accumulation of amyloid beta-peptide (Aβ) in amyloid plaques and the walls of blood vessels (cerebral amyloid angiopathy or CAA). A great deal of evidence supports the amyloid hypothesis that states that deposition/accumulation of Aβ in the brain is a causal event leading to dementia in AD [1]. Therefore, preventing and clearing the Aβ accumulation in the brain has been considered to be prophylactic and therapeutic, respectively. Because active and passive Aβ immunization is highly effective in preventing and clearing brain Aβ accumulation in animal models of AD, Aβ immunotherapy emerged as one of the most promising approaches for AD prevention and therapy [2-4]. Human clinical trials of synthetic Aβ vaccination (AN-1792), however, were halted due to brain inflammation presumably induced by T-cell-mediated and/or Fc-mediated immune responses [5, 6] and/or toxicity of AN1792 [7-9]. Thus, the active immunization may cause T-cell mediated inflammation and Aβ-IgG complexes are likely to cause Fc-mediated microglial activation resulting in production of pro-inflammatory cytokines, chemokines and reactive oxygen species. Additionally, these Aβ immunotherapies were often associated with vasogenic edema and microhemorrhages in the brain [10-13]. The latter was thought to be caused by relocation of parenchymal Aβ aggregates to the walls of cerebral blood vessels [14, 15]; thus, the inflammatory responses and cerebral hemorrhages associated with Aβ immunotherapies can be detrimental to the AD patients' health. Indeed, recent clinical trials of passive Aβ immunotherapies failed to meet their primary end-points [16]. We hypothesize that the beneficial effects of Aβ immunotherapies are counteracted by inflammatory responses and cerebral hemorrhages associated with their intrinsic attributes.

Low levels of naturally occurring autoantibodies to Aβ are found in AD patients as well as healthy humans [17-20]. We previously reported naturally occurring IgM class human autoantibodies which hydrolyze Aβ and inhibit aggregation and neurotoxicity of Aβ [21]. We isolated and characterized many clones of immunoglobulin variable domains (IgVs) with Aβ-hydrolysis activity by screening a human IgV library [22]. One of such IgV clones with exceptionally high potency and specificity in Aβ hydrolysis consisted of a single domain IgV containing only one V_L domain (designated IgV_L5D3). The structures and amino acid sequences of IgV_L5D3 was previously reported [22] (GenBank FJ231718). The catalytic sites of IgVs are structurally similar to those of serine proteases and serine protease-like catalytic triads have been identified in the V domains of IgVs [23, 24]. The catalytic mechanism of IgVs involves nucleophilic attack on the electrophilic carbonyl of peptide bonds. IgV_L5D3 hydrolyzes Aβ at rates superior to naturally occurring Igs by 3-4 orders of magnitude and mainly cuts the His14-Gln15 bond and, less often, other peptide bonds located in the central Aβ region [22]. The *k*cat of IgV_L5D3 is comparable with that of neprilysin, Aβ degrading enzyme [22]. Expression of neprilysin in neurons and skeletal muscle via rAAV-mediated gene delivery is effective in reducing brain Aβ load in AD mouse models [25, 26]. A conventional, single IgG binds and inactivates only two Aβ molecules while one molecule of proteolytic Igs can hydrolyze/inactivate thousands of Aβ molecules. The catalytic IgVs permanently degrade Aβ into smaller fragments, Aβ1-14 and Aβ15-40 or Aβ15-42 [22]. These cleaved fragments do not form amyloid and are not toxic to

neurons [27, 28]. Because such smaller Aβ fragments are not involved in formation of Aβ aggregates [27, 28] and because catalytic IgVs lack the Fc region and do not form a stable IgV-antigen complex, it is unlikely to produce the side effects such as inflammation, cerebral amyloid angiopathy, and hemorrhage. Thus, the catalytic IgVs can be superior to non-catalytic Igs in therapeutic efficacy and safety. Here, we evaluated the prophylactic and therapeutic efficacy and safety of brain-targeted IgV_L5D3 gene delivery via recombinant adeno-associated virus serotype 9 (rAAV9) in an AD mouse model (TgAPPswe/PS1dE9).

Materials and Methods

Ig Expression Vector Construction

A catalytic IgV_L clone, 5D3, composed of a single variable light chain domain (IgV_L) was previously isolated and characterized [21]. IgV_L5D3 catalyzes the hydrolysis of Aβ specifically and does not contain the Fc region. An rAAV expression vector for IgV_L5D3, pAAV-CAIgV_L5D3, was constructed by replacing cDNA for scFv59 with IgV_L 5D3 cDNA in pAAV-CAscFv59 [29] and by inserting the 530 bp rabbit β-globin 3' non-coding sequence (βG3') from pCAGGS [30] as a stuffer into the 5' side of the 3' inverted terminal repeat for optimal encapsidation of rAAV (Fig. 1). The expression plasmid contained the cytomegalovirus enhancer/β-actin promoter for high expression, the signal sequence of the immunoglobulin heavy chain gene for secretion, and the woodchuck hepatitis virus post-transcriptional regulatory element for enhanced translation efficiency. IgV_L5D3 contained Myc-His tag at the C-terminal ends as markers.

Expression and Secretion of IgV_L5D3 in HEK293 Cells

Human embryonic kidney (HEK) 293 cells were cultured in Dulbecco's modified Eagle's medium (DMEM) supplemented with 10 % fetal bovine serum in 6 cm dishes and transfected with 5 μg of pAAV-CAIgV_L5D3 using GenJet In Vitro DNA transfection reagent (SignaGen Laboratories, Rockville, MD, USA) according to the manufacturer's protocol. Seventy-two hours after transfection, the media and cells were harvested, and the proteins in the media and cells were separated by 10-20 % SDS-PAGE. After electrotransfer to polyvinylidine difluoride (PVDF) membranes (Millipore, Bedford, MA, USA), IgV_L5D3 was detected by anti-c-Myc monoclonal antibody (Sigma, St. Louis, MO, USA) and visualized by the enhanced chemiluminescence method (Amersham, Arlington Heights, IL, USA) according to the manufacturers' protocols.

Recombinant Adeno-associated Virus Preparation

Using the calcium phosphate method as previously described [31], HEK293 cells were transfected with the helper plasmids containing the AAV2 rep and AAV9 capsid gene and pAAV-CAIgV_L5D3 to produce pseudotyped rAAV9 encoding IgV_L5D3. Produced viral particles were released from the cells by rapid freeze and thaw and separated by iodixanol gradient fractionation. The viral particles were further purified by a HiTrap Q column using an ATKA FPLC system (GE Healthcare, Piscataway, NJ, USA) as previously described [32]. The titer of rAAV virion that contained the vector genomes was determined by the quantitative dot-blot assay as described previously [33].

Experimental Animals and Stereotaxic Injection of rAAVs

C57BL/6J mice and an AD mouse model, B6.Cg-Tg(APPswe, PSEN1dE9) 85Dbo/J mice (here referred to as TgAPPswe/PS1dE9 mice) [34] purchased from Jackson Laboratory, were used to study the prophylactic and therapeutic efficacy of intracerebroventricular injection of rAAV9-IgV_L5D3. Mice were anesthetized by pentobarbital and placed on a stereotaxic instrument with a motorized stereotaxic injector (Stoelting, Wood Dale, IL, USA). A midline incision was made to expose the bregma. A hole in the skull was made by a drill 0.5 mm posterior to the bregma and 1.0 mm right to the midline. rAAV [3.0×10^{10} vector genomes (vg) in 10 μl PBS/mouse] was injected unilaterally into the right ventricle at the depth of 2 mm at a rate of 1 μl/min. After allowing the needle to remain in place for 5 min, the needle was slowly raised at a rate of 0.1 cm/min. For the prophylactic study, 2-month-old mice were injected with a single dose of rAAV9-IgV_L5D3 as described above and, 8 months after the injection, subjected to cerebrospinal fluid (CSF) collection. For the therapeutic study, rAAV9-IgV_L5D3 injections were carried out at 10 months of age and, 5 months after the injections, mice were subjected to CSF collection. Upon the completion of the CSF collection, mice were terminated for immunohistochemical and biochemical analyses. As controls, mice were similarly injected with PBS. The numbers of mice, their sexes, genotypes, and mortality are summarized in Table 1 (prophylaxis) and Table 2 (therapy). All animal protocols used for this study were prospectively reviewed and approved by the Institutional Animal Care and Use Committee of the University of Illinois College of Medicine at Peoria.

Murine CSF Isolation

Cerebrospinal fluid was isolated from the cisterna magna compartment using the method described by DeMattos et al. [35]. Mice were anesthetized by pentobarbital and fixed face down on a narrow platform. An incision was made from the top of the skull to the dorsal thorax. The musculature from the base of the skull to the first vertebrae was carefully removed to expose the meninges overlying the cisterna magna. The surrounding area was gently cleaned with 1× PBS using cotton swabs to remove any residual blood or other interstitial fluid. The arachnoid membrane covering the cistern was punctured with a 29 gauge insulin syringe. A polypropylene narrow bore pipette was immediately placed in the hole to collect CSF. As the primary CSF exiting the compartment was collected, a second collection was performed after the cistern was refilled within 2 min. About 10 to 15 μl CSF was collected from each mouse.

Immunohistochemical and Histochemical Analyses

Mice were deeply anesthetized with pentobarbital and cardinally perfused with cold PBS and the brains were quickly removed. The neocortices and hippocampi of the left hemispheres were separately dissected and stored in −80 °C for further studies. The right hemispheres were fixed in 4 % paraformaldehyde for 48 h. For some mice, both hemispheres were fixed in 4 % paraformaldehyde for 48 h for immunohistochemical analysis. The brains were then stored overnight in 30 % sucrose in 0.1M PBS and frozen in Tissue-Tek optimal cutting temperature compound. Coronal sections (35 μm thick) of the brains were cut on a freezing-stage cryotome and kept in 0.1 M PBS at 4 °C. Sections were

subjected to immunohistochemical and histochemical staining. The brain sections were immunostained with anti-c-Myc monoclonal antibody (Sigma) for detection of IgV_L5D3. The Aβ deposit in the brain was detected by 6E10 antibody (Covance, Princeton, NJ, USA). Neuroinflammation was detected by rabbit anti-mouse Iba1 (Wako, Osaka, Japan), rat anti-mouse CD11b, rat anti-mouse CD45 and rabbit anti-mouse GFAP antibodies (Serotec, Oxford, UK). Free floating immunohistochemistry was performed by using avidin-biotin immunoperoxidase method (Vector, Burlingame, CA, USA). Endogenous peroxidase was eliminated by treatment with 1 % H_2O_2/10 % methanol Tris-buffered saline (TBS) for 60 min at room temperature. After washing with 0.1 M Tris buffer (pH 7.5) and 0.1 M TBS (pH 7.4), sections were blocked with 5 % normal serum (from the same animal species in which the secondary antibody was made) in 0.1M TBS with 0.5 % triton-X-100 (TBS-T) for 60 min at room temperature to prevent non-specific protein binding. The sections were then incubated with primary antibodies as described above in 2 % serum in TBS-T for 18-48 h at 4 °C. For the negative controls, slides were processed without primary antibody. The sections were rinsed in 0.1 M TBS and incubated with biotinylated secondary antibodies in 2 % serum TBS-T for 2 h at room temperature. Finally, the avidin biotin peroxidase method using 3,3'-diaminobenzidine as a substrate (Vector) was performed. Some sections were counterstained with hematoxylin.

For detection of fibrillar Aβ plaque, tissue sections were stained in 1 % thioflavin S (Sigma) and rinsed with 70 % ethanol. After washing with H_2O, the sections were mounted in 75 % glycerol in H_2O.

To detect possible cerebral hemorrhages, Prussian blue reaction was carried out on brain sections using an Iron Stain kit (Sigma-Aldrich, St. Louis, MO, USA) according to the manufacturer's protocol.

Histomorphometry was performed for quantification of amyloid deposits and reactive/activated glial cells using an Olympus BX61 automated microscope, Olympus Fluoview system and Image Pro Plus v4 image analysis software (Media Cybernetics, Silver Spring, MD, USA) capable of color segmentation and automation via programmable macros. Five coronal brain sections, each separated by an approximately 400 μm interval, starting at 1.3 mm posterior to the bregma to caudal, from each mouse were analyzed. Both neocortex and hippocampus were found in all the brain sections and analyzed separately. Stained areas were expressed as a percentage of total neocortex or hippocampus, respectively. For CAA, thioflavin S positive blood vessels in 3 to 4 right hemisphere sections for each mouse were enumerated and expressed as a number of thioflavin S-positive blood vessels per square millimeter. Data were expressed as mean±standard error of the mean (SEM).

Quantification of Brain and CSF Aβ by ELISA

The left neocortex and hippocampus were removed from storage at −80 °C, lysed using the Bio-Plex cell lysis kit (Bio-Rad Laboratories, Hercules, CA, USA) and homogenized according to the manufacturer's protocol, and centrifuged at 16,000×g for 30 min at 4 °C. The supernatants containing buffer-soluble Aβ were collected and the protein concentrations in the supernatants were determined by Bio-Rad Protein Assay (Bio-Rad). The pellets containing buffer-insoluble Aβ were further dounce homogenized in guanidine

hydrochloride (final concentration, 5 M) and then rock-shaken for 3–4 h at room temperature. Levels of buffer-soluble and insoluble Aβ in the left neocortex and hippocampus and Aβ in the CSF were quantified by Aβ42 and Aβ40 enzyme-linked immunosorbent assay (ELISA) kits (Invitrogen, Carlsbad, CA, USA) according to the manufacturer's protocol, in which antibody to the N-terminous of human Aβ had been coated.

Immunoblotting for Detection of IgV_L5D3 Expression and Neuroinflammation in the Brain

Buffer-soluble homogenates (50 μg) from the hippocampus and neocortex or CSF samples (10 μl) were mixed with 2 × sample buffer (final concentration: 60mM Tris-HCl, 2 % SDS, 10 % glycerol, 0.001 % bromphenol blue, pH: 6.8) and heated at 100 °C for 5 min. Samples were subjected to 10-20 % Tris-HCl gradient SDS-PAGE and electrotransferred to PVDF membranes. IgV_L5D3 on the membranes were detected using anti-c-Myc monoclonal antibody. Neuroinflammation was detected by rat anti-mouse CD45 and rabbit anti-mouse GFAP antibodies. Then, specific bands were visualized by an enhanced chemiluminescence system (Amersham, Arlington Heights, IL, USA) according to the manufacturer's protocol. For CD45 and GFAP quantification, the membranes were reprobed with anti-glyceraldehyde-3-phosphate dehydrogenase (GAPDH) antibody (Chemicon, Temecula, CA, USA). The optical densities of protein bands from the membranes were determined by densitometric scanning using an HP Scanjet G3010 Photo Scanner and Image J V1.40 (National Institutes of Health, MD, USA). The optical density of each protein band was divided by that of the GAPDH band on the same lane from the same membrane for normalization.

Determination of Anti-IgVL5D3 Antibody Titers in Sera

In order to determine levels of anti-IgV_L5D3 antibodies which might be possibly increased in mice subjected to rAAV-IgV_L5D3 injection, blood was drawn from mice 4 and 7 months and 2 and 5 months after rAAV injections for the prophylactic and therapeutic studies, respectively. Approximately 100 μl of blood per mouse was taken from the tail vein, incubated at room temperature for 1 h and then transferred to 4 °C. After overnight incubation, blood was centrifuged at 12,000 × g for 30 min and serum was stored at –80 °C and thawed at the time of assay. ELISA was carried out to determine titers of anti-IgV_L5D3 antibodies. Briefly, 96-well plates were coated with 250 ng of purified IgV 5D3 per well at 4 °C overnight, followed by incubation with blocking buffer (1× PBS containing 0.5 % BSA, 0.05 % Tween-20 and 5 % goat serum) at room temperature for 1 h. Then, diluted serum samples (1:50) were added to the microtiter wells and incubated at 4 °C overnight. The next day, the microplates were washed 5 times using washing buffer (1× PBS containing 0.05 % Tween-20), and then incubated with HRP-conjugated secondary antibody at room temperature for 1 h. The microplates were then washed with washing buffer 5 times followed by incubation with 3,3’,5,5’-tetramethylbenzidine (TMB) (Kirkegaard & Perry Laboratories Inc., Gaithersburg, MD, USA) for 15 min to allow the development of color. The reaction was stopped by adding 100 μl of 1 N H_2SO_4. The optical densities were determined at 450 nm using a Microplate Reader. Serial dilutions of anti-c-Myc antibody were used as standard to determine titers of anti-IgV_L5D3 antibodies.

Statistical Analysis

Data were expressed as mean ± SEM. Analysis of variance (ANOVA) and two-tailed Student's t-test were used to determine the intergroup significant difference. $P < 0.05$ was considered statistically significant.

Results

Secretion of IgV_L5D3 from HEK293 Cells

In order to confirm secretion of IgVs from mammalian cells, cultured HEK293 cells were transfected with expression vectors, pAAV-CAIgV_L5D3 and 72 h later, 40 μg of cell lysate and 15 μl of the conditioned medium were separated by 4–15 % SDS-PAGE and immunoblot analysis was performed to identify IgVs using anti-c-Myc antibody. IgV_L5D3 contains the c-Myc sequence (EQKLISEEDL) as a marker. IgV_L5D3 was detected as approximately 18 kDa fragments in cell lysate and medium (Fig. 2). Thus, IgV_L5D3 was expressed in HEK293 cells and secreted into the medium.

Treatments and Mortality

To investigate the prophylactic effects of brain-targeted IgV_L5D3 expression, rAAV9-IgV_L5D3 (3×10^{10} vg/mouse in 10 μl PBS) was injected into the right lateral brain ventricles of TgAPPswe/PS1dE9 mice and their non-transgenic littermates (Non-Tg mice) at 2 months of age. PBS was similarly injected into control mice. To investigate the therapeutic effects, rAAV9-IgV_L5D3 (3×10^{10} vg/mouse) or PBS (controls) was similarly injected to TgAPPswe/PS1dE9 and Non-Tg mice at 10 months of age. The mice were euthanized at 10 and 15 months of age for prophylaxis and therapy, respectively. The numbers of mice, their genotypes, sexes, treatments, and the numbers of dead mice during the experimental courses are summarized in Table 1 (prophylaxis) and Table 2 (therapy). There was no difference in the mortalities between any treatment groups (chi square test, $P > 0.05$). A high mortality rate of TgAPPswe/PS1dE9 mice with a death peak around 3 to 4 months of age due to seizures was previously reported [36].

Stable Strong Expression of IgV_L5D3 in the Hippocampus but Variable Expression of IgV_L5D3 in the Neocortex and CSF

To determine the expression areas and levels 8 (prophylaxis) and 5 (therapy) months after rAAV injections, brain sections were stained with anti-c-Myc antibody for IgV_L5D3 expression using the avidin-biotin-peroxidase method. IgV_L5D3 has a myc sequence as a marker at the C-terminal end. One single injection of rAAV9-IgV_L5D3 into the right lateral ventricle of TgAPPswe/PS1dE9 mice resulted in widespread, high expression of IgV_L5D3 in the right hippocampus but its expression in the neocortex showed great variability among different mice. IgV_L5D3 expression in the left hemisphere was limited to the anterior half of the hippocampus. Brain sections from a representative mouse from the therapeutic group are shown in Fig. 3. At higher magnifications, strong immunereactivity for IgV_L5D3 was found in both neuronal cell bodies and the neuropil in the neocortex and hippocampus (Supplemental Fig. 1b and c), suggesting intracellular accumulation of IgV_L5D3 and its secretion from the cells, respectively. Some ependymal cells in the choroid plexus showed

strong immunoreactivity for IgV_L5D3 (Supplemental Fig. 1a), suggesting secretion of IgV_L5D3 into the CSF from the cells. There was no difference in the expression patterns between the prophylactic and therapeutic groups.

To further determine the expression levels of IgV_L5D3 in the left hippocampus, neocortex, and CSF, immunoblot analysis was performed using samples from the therapeutic group. Expressed IgV_L5D3 was detected with anti-c-Myc antibody (Fig. 4). Strong high density bands of IgV_L5D3 are identified as an approximately 18 kDa fragment in the left hippocampus in every mouse subjected to rAAV9-IgV_L5D3 injection (Fig. 4). However, there was great variability in the IgV_L5D3 expression levels in the left neocortices among different mice subjected to rAAV9-IgV_L5D3 injection (Fig 4). Moderately variable levels of IgV_L5D3 expression was identified in the CSF isolated from the mice subjected to rAAV9-IgV_L5D3 injections (Fig. 4). Thus, variability was observed in levels of IgV_L5D3 expression in the left neocortex and CSF in the mice subjected to rAAV9-IgV_L5D3 injections.

IgV_L5D3 Brain Expression via Prophylactic rAAV9 Injection Reduces Aβ Load in the Right Hippocampus

Eight months after rAAV9-IgV_L5D3 or PBS injection, mice were terminated at age 10 months. Diffuse and fibrillar Aβ deposits in the right brain hemispheres were visualized by 6E10 antibody (Fig. 5a) and fibrillar Aβ deposits were identified by thioflavin S fluorescence (Fig. 5c). The visualized areas were quantified by morphometric analysis and expressed as the percentage of area positive for Aβ immunohistochemistry or thioflavin fluorescence. The average Aβ loads in right hippocampus by 6E10 immunoreactivity were 0.315±0.030 and 0.470±0.058 % for mice treated with rAAV9-IgV_L5D3 and PBS, respectively (Fig. 5b). The average Aβ loads in right neocortex by 6E10 immunoreactivity were 0.541±0.065 and 0.868±0.096 % for mice treated with rAAV9-IgV_L5D3 and PBS, respectively (Fig. 5b). Thus, prophylactic injection of rAAV9-IgV_L5D3 reduced the Aβ-immunoreactive deposits in the right hemisphere compared with PBS injection ($p = 0.03$ for the hippocampus and $p = 0.01$ for the neocortex). In the right hippocampus, the average amyloid load by thioflavin S fluorescence in rAAV9-IgV_L5D3-treated mice (0.22±0.04 %) was significantly less than that in PBS-treated mice (0.36±0.05 %, $p = 0.04$) (Fig. 5d). Although, in the right neocortex, the average amyloid load by thioflavin fluorescence in rAAV9-IgV_L5D3-treated mice (0.36±0.07 %) was less than that in PBS-treated (0.45±0.06 %, $p = 0.24$) mice, the difference was not significant. Thus, prophylactic rAAV9-IgV_L5D3 injection reduced the Aβ load in the right hippocampus by approximately 20 to 40 % as compared with PBS injection. The reasons for the discrepancy in Aβ load in the right neocortex between 6E10 immunoreactivity and thioflavin fluorescence are not clear but may be due to the small numbers of experimental animals or the greater variability in the expression levels of IgV_L5D3 in the neocortex, or both.

Levels of buffer-soluble and insoluble Aβ in the left hippocampus and neocortex of the transgenic mouse groups were quantified by Aβ42- and Aβ40-specific ELISA. No differences were found between the groups in buffer-soluble and insoluble Aβ levels (data not shown).

IgV_L5D3 Brain Expression via Prophylactic rAAV9 Injection does not Increase Inflammation

Aβ immunotherapy may induce brain inflammation. Eight months after rAAV9-IgV_L5D3 and PBS injection, activated microglia/monocytes in the right hippocampus and neocortex were immunostained with anti-Iba1 and anti-CD45 antibodies (Fig. 6a and c). The visualized areas were quantified by morphometric analysis and expressed as the percentage of area positive for Iba1 or CD45 immunostaining. There were no differences in expression levels of these markers of microglial/myeloid cells in the right hippocampus and neocortex between any transgenic groups (Fig. 6b and d).

Inflammatory responses possibly induced by rAAV9-mediated IgV_L5D3 brain expression were studied by determining expression levels of proinflammatory cytokines by ELISA in the left neocortex. On average, expression levels of IL-1β, IL-6, and TNF-α in the rAAV9-IgV_L5D3-injected transgenic group were lower than those in the PBS-injected transgenic group. However, the differences were not significant (Fig. 6e).

Infiltration of inflammatory cells was not observed in the brain sections in any of the treatment groups. Thus, there was no evidence of an increase in inflammatory responses due to the prophylactic rAAV9-IgV_L5D3 treatment.

IgV_L5D3 Brain Expression via Therapeutic rAAV9 Injection Reduces Aβ-immunoreactive Deposits in the Right Hippocampus and Fibrillar Aβ Deposits in the Right Neocortex

Five months after rAAV9-IgV_L5D3 or PBS injection, mice were terminated at age 15 months. Diffuse and fibrillar Aβ deposits in the right brain hemispheres were visualized by anti-Aβ 6E10 antibody (Fig. 7a) and fibrillar Aβ deposits were detected by thioflavin S fluorescence (Fig. 7c). The visualized areas were quantified by morphometric analysis. Aβ immunoreactive areas in the right hippocampus reduced in the rAAV9-IgV_L5D3-treated transgenic group (1.38±0.09 %) compared to the PBS-treated transgenic group (1.86±0.13 %, $p = 0.02$) but the reduction in the neocortex in the rAAV9-IgV_L5D3-treated group was not significant (1.97±0.11 for IgV_L5D3 and 2.32±0.19 for PBS, $p = 0.19$) (Fig. 7b). Thioflavin S-positive areas in the right neocortex in the rAAV9-IgV_L5D3-treated transgenic group (0.69±0.04 %) significantly decreased compared to those in the PBS-treated transgenic group (0.88±0.05 %, $p = 0.03$) but the reduction in the right hippocampus in the rAAV9-IgV_L5D3-treated transgenic group barely missed its significance (0.47±0.05 for IgV_L5D3 and 0.62±0.06 for PBS, $P = 0.09$) (Fig. 7d). The reasons for the discrepancies in Aβ load between Aβ-immunoreactivity and thioflavin S fluorescence are not clear but probably due to varying levels of IgV_L5D3 expression and the small numbers of experimental animals. Thus, brain-targeted IgV_L5D3 expression via therapeutic rAAV9 injection reduced Aβ-immunoreactive deposits in the right hippocampus and fibrillar Aβ deposits in the right neocortex.

IgV_L5D3 Brain Expression via Therapeutic rAAV9 Injection does not Reduce Levels of Buffer-soluble and Insoluble Aβ in the Left Hemisphere

Levels of buffer-soluble and insoluble Aβ in the left hippocampus and neocortex of the transgenic mouse groups subjected to therapeutic rAAV9-IgV_L5D3- and PBS-treatments

were similarly determined by ELISA. No differences were found between the two treatment groups in buffer-soluble and insoluble Aβ levels (data not shown).

IgV_L5D3 Brain Expression via Therapeutic rAAV9 Injection Reduces Microglia/monocyte Activation

Brain sections were stained with anti-Iba1 antibody for activated microglia and Iba1-immunoreactive areas were quantified by morphometric analysis (Fig. 8a and b). Iba1-immunoreactive areas in the rAAV9-IgV_L5D3-treated transgenic group (0.27±0.03 and 0.33±0.03 % for the right hippocampus and neocortex, respectively) decreased compared to the PBS-treated transgenic group (0.41±0.03, $p = 0.02$ and 0.44±0.03 %, $p = 0.04$ for the right hippocampus and neocortex, respectively). CD45 expression levels in the left hemisphere were determined by immunoblot analysis (Fig. 8c and d). CD45 expression levels in the rAAV9-IgV_L5D3-treated transgenic group (1.10±0.01 and 0.34±0.02 for the left hippocampus and neocortex, respectively) were lower than those in the PBS-treated transgenic group (1.22±0.07 and 0.49±0.04 for the right hippocampus and neocortex, respectively, $p = 0.02$ for both). Thus, brain-targeted IgV_L5D3 expression via therapeutic rAAV9 injection reduced Iba1-positive microglia in the right hemisphere and CD45 expression levels in the left hemisphere.

Inflammatory responses possibly induced by therapeutic rAAV9-IgV_L5D3 treatment were also studied by determining expression levels of IL-1β, IL-6, and TNF-α by ELISA in the left neocortex. On average, expression levels of IL-1β, IL-6, and TNF-α in the rAAV9-IgV_L5D3-injected transgenic group were lower than those in the PBS-injected transgenic group. However, the differences were not significant (Fig. 8e).

IgV_L5D3 Brain Expression via Therapeutic rAAV9 Injection does not Cause Increases in Cerebral Amyloid Angiopathy and Microhemorrhages

Aβ-immunotherapy can cause hemorrhages which are often accompanied by an increase in CAA. Therefore, we enumerated the numbers of blood vessels positive for thioflavin S fluorescence and of hemorrhages detected by Prussian blue reaction. No differences were found in CAA (Fig. 9) and hemorrhages (data not shown) between the rAAV9-IgV_L5D3-treated and PBS-treated transgenic groups.

Anti-IgV_L5D3 Antibodies Induced by Brain-targeted IgV_L5D3 Expression via rAAV9 were Negligible

IgV_L5D3 is derived from human Ig and can induce immune responses in mice. To determine whether brain-targeted IgV_L5D3 expression via rAAV9 elicits anti-IgV_L5D3 antibody production, blood was prepared from rAAV9-IgV_L5D3-treated transgenic mice at 4 and 7 months after rAAV9 injection for the prophylactic group and at 2 and 5 months after the injection for the therapy group. Their serum titers were determined by ELISA. Out of 8 mice in the prevention group, 3 mice had anti-IgV_L5D3 titers ranging from 1 to 21 ng/ml and all mice in the therapy group had titers ranging from 14 to 112 ng/ml (Fig. 10). Thus, their titers were modest and appeared to have insignificant effects on inactivating IgV_L5D3 because CSF levels of IgV_L5D3 were estimated to be more than 1 μg/ml based on immunoblotting of CSF (Fig. 4).

Discussion

Anti-Aβ immunotherapy has been repeatedly demonstrated to be effective in reducing brain Aβ levels in animal models and clinical trials [37, 38]. However, human clinical trials of active immunization with aggregated Aβ (AN1792) were halted due to brain inflammation, presumably induced by T-cell-mediated and/or Fc-mediated immune responses [5, 6]. Additionally, the clinical trials and passive immunization (anti-Aβ antibody administration) induced CAA and microhemorrhages in an AD patient [39] and some AD mouse models [14, 15, 40]. Because Aβ deposits in CAA increased only in the specific brain area where the highest extent of parenchymal amyloid plaque clearance was observed, one of the mechanisms explaining the increased hemorrhage after anti-Aβ immunotherapy is that Aβ in parenchymal amyloid plaques is solubilized by anti-Aβ antibody and focally relocated to the blood vessels [41, 42]. Most recent results from the clinical trials of passive immunization (bapineuzumab) have not produced significant clinical benefits in a wide range of AD patients [43, 44]. We hypothesize that the beneficial effects of Aβ clearance by active and passive anti-Aβ immunization are reduced by harmful proinflammatory responses that are induced by IgG-Aβ immune complex-mediated and/or Fc receptor-mediated activation of immune cells [10, 45]. Because Aβ-specific catalytic IgVs lack the Fc region and cannot form a stable IgV-Aβ complex, it is highly probable that catalytic IgVs do not induce harmful immune responses. Furthermore, because the catalytic IgVs permanently degrade Aβ into smaller fragments that are less likely to form aggregates, they circumvent Aβ vascular deposits and hemorrhages. Therefore, we hypothesize that a safe and effective immune therapy for AD can be established by use of Aβ-specific catalytic IgVs.

We previously isolated and characterized a single chain antibody, scFv59, consisting of an antibody heavy chain variable domain linked by a flexible polypeptide linker to a light chain variable domain [46]. scFv59 specifically binds with Aβ aggregates. As reported previously, we injected rAAV5 encoding scFv59 (rAAV5-scFv59) into the right lateral ventricles of 10-month-old TgAPPswe/PS1dE9 mice and determined the efficacy and safety of the therapeutic modality 5 months after the injection. The therapeutic injection of rAAV5-scFv59 reduced Aβ load in the hippocampus but caused hemorrhages that were associated with a focal increase in blood vessel amyloid [29]. In line with our hypothesis, prophylactic and therapeutic injection of rAAV9-IgV_L5D3 into the right lateral ventricles of TgAPPswe/PS1dE9 mice reduced Aβ load without causing CAA, hemorrhages and inflammation.

Cells in the brain can be transduced by rAAV vectors and long-term expression of a transgene can be achieved. Levels of transgene expression, target cell types, and transduced regions vary depending upon rAAV serotypes. In the previous experiments, we used rAAV serotype 5 for intracranial delivery of scFv59 after optimization of scFv59 brain expression by testing 3 different pseudotyped rAAVs (serotype 1, 2, and 5) [47]. Widespread and high expression of scFv59 was observed in the hippocampi in both hemispheres in rAAV5-injected mice but expression of scFv59 in the neocortex was limited and less intense than that of the hippocampus. Immunoreactivity for scFv59 was found in both neuronal cell bodies and the neuropils. Although scFv59 was readily detectable in the hippocampus and CSF by immunoblotting, scFv59 was undetectable in the neocortex by the same method. Here, we utilized rAAV serotype 9 (rAAV9) for IgV_L5D3 brain expression because our

preliminary results with a limited number of mice indicated higher expression levels of a transgene by rAAV9 than the other serotypes (1, 2, 5, and 8) (data not shown) and because widespread robust expression by rAAV9 in the brain has been reported [48-51]. A single rAAV9 injection into the right lateral ventricle transduced the entire right hippocampus. Although expressed IgV_L5D3 in the left hippocampus and neocortex was readily discernible in all mice by immunoblot analysis, the transduced area in the left hippocampus was limited to the anterior half of the hippocampus by immunohistochemistry (Fig. 3 and 4). Expression of IgV_L5D3 was limited to small areas in both the right and left neocortex (Fig. 3) and levels of IgV_L5D3 expression largely varied from mouse to mouse (Fig. 4). Thus, the expression pattern of IgV_L5D3 by rAAV9 was similar to that of scFv59 by rAAV5 but expression levels of IgV_L5D3 by rAAV9 appeared to be higher than that of scFv59 by rAAV9 as exemplified by immunoblot analysis of the neocortex. The significant reductions in Aβ load were more consistently found in the right hippocampus than the right neocortex, probably due to varying IgV_L5D3 expression levels in the neocortex resulting in a large fluctuation in Aβ load, and no reductions were found in the left hemisphere. Thus, the reductions in Aβ load largely matched with the IgV_L5D3 expression pattern. In the future, a side-by-side comparison of scFv59 and IgV_L5D3 by performing direct intraparenchymal injections of the antibodies in AD mouse models will assess their precise differences in the Aβ clearance efficacy and safety.

Unexpectedly, the prophylactic injection of rAAV9-IgV_L5D3 did not reduce activation of microglia/macrophages in the right hemisphere even though Aβ load in the right hemisphere was reduced. As we expected, however, the therapeutic injection of rAAV9-IgV_L5D3 reduced activated microglia/macrophages in the right hippocampus and neocortex, indicating that IgV_L5D3 does not activate microglia/macrophages. During aging, microglia show diminished capacity for normal functions including elimination of toxic substances and pathogens and regulation of tissue injury and repair [52]. Indeed, microglia isolated from 6-month-old AD mouse models (TgPS1M146L/APP751SL) show an alternative activation state with Aβ phagocytic capabilities and those from 18-month-old AD mouse models display a classic cytotoxic phenotype [53]. Thus, the discrepancy in the microglia/macrophage activation status between the prophylactic and therapeutic modalities may be due to the microglial phenotypic changes during aging.

IgV_L5D3 was isolated from a human IgV library and contains a Myc-His tag. Therefore, IgV_L5D3 can induce its antibodies in mice, resulting in neutralization of its anti-Aβ catalytic activity. Injection of rAAV9-IgV_L5D3 into the lateral ventricles of TgAPPswe/PS1dE9 mice elicited modest anti-IgV_L5D3 titers of less than 1 nM. The anti-IgV_L5D3 titers are very similar to those against scFv59 previously observed when rAAV5-scFv59 was injected into the ventricles of TgAPPswe/PS1dE9 mice [47]. Because 1 % or less antibodies in the circulation can cross the blood-brain barrier [54, 55], such modest levels of anti-IgV_L5D3 titers will probably have no significant effect on its catalytic activity.

Neprilysin is a metalloproteinase and efficiently degrades Aβ. Expression of neprilysin in the brain via rAAV reduced Aβ load in AD mouse models [26, 56, 57]. IgV_L5D3 exceeds neprilysin in the efficacy (kcat 2.2 vs 6.3/min) and specificity [22, 58]. Intracranial expression of IgV_L5D3 via rAAV9 reduced the cerebral Aβ load without inducing brain

inflammation, cerebral hemorrhages, and exacerbation of CAA. Therefore, intracranial IgV_L5D3 delivery may be a safer and more efficacious approach to prevent and treat AD.

Our experimental results indicate that higher and more widespread expression of IgV_L5D3 is required for more widespread and robust reduction of Aβ load in the brain. Self-complementary rAAV vectors can significantly improve the efficacy of transduction as compared with identical vectors in a single-stranded format [59-61] . Widespread and high expression of transgenes in the brain has been reported by systemic intravenous injection of rAAV9 [62], intraparenchymal injection of rAAV9 into nuclei with divergent connections [49], and their combinations [63]. These strategies for improved gene therapy should be exploited in future.

Supplementary Material

Refer to Web version on PubMed Central for supplementary material.

Acknowledgements

This work was supported in part by grants from the National Institutes of Health (AG037814, AG030399, and EY018478). We thank Dr. James Wilson at University of Pennsylvania for providing pAAV9 packaging plasmid and Ms. Linda Walter for assistance in preparation of this manuscript.

References

1. Hardy J. Amyloid double trouble. Nat Genet. 2006; 38:11–12. [PubMed: 16380721]
2. Schenk D, Barbour R, Dunn W, Gordon G, Grajeda H, Guido T, Hu K, Huang J, Johnson-Wood K, Khan K, et al. Immunization with amyloid-beta attenuates Alzheimer-disease-like pathology in the PDAPP mouse. Nature. 1999; 400:173–177. [PubMed: 10408445]
3. Janus C, Pearson J, McLaurin J, Mathews PM, Jiang Y, Schmidt SD, Chishti MA, Horne P, Heslin D, French J, et al. A beta peptide immunization reduces behavioural impairment and plaques in a model of Alzheimer's disease. Nature. 2000; 408:979–982. [PubMed: 11140685]
4. Morgan D, Diamond DM, Gottschall PE, Ugen KE, Dickey C, Hardy J, Duff K, Jantzen P, DiCarlo G, Wilcock D, et al. A beta peptide vaccination prevents memory loss in an animal model of Alzheimer's disease. Nature. 2000; 408:982–985. [PubMed: 11140686]
5. Check E. Nerve inflammation halts trial for Alzheimer's drug. Nature. 2002; 415:462. [PubMed: 11823817]
6. Orgogozo JM, Gilman S, Dartigues JF, Laurent B, Puel M, Kirby LC, Jouanny P, Dubois B, Eisner L, Flitman S, et al. Subacute meningoencephalitis in a subset of patients with AD after Abeta42 immunization. Neurology. 2003; 61:46–54. [PubMed: 12847155]
7. Sigurdsson EM, Wisniewski T, Frangione B. A safer vaccine for Alzheimer's disease? Neurobiol Aging. 2002; 23:1001–1008. [PubMed: 12470795]
8. Hock C, Konietzko U, Papassotiropoulos A, Wollmer A, Streffer J, von Rotz RC, Davey G, Moritz E, Nitsch RM. Generation of antibodies specific for beta-amyloid by vaccination of patients with Alzheimer disease. Nat Med. 2002; 8:1270–1275. [PubMed: 12379846]
9. Bayer AJ, Bullock R, Jones RW, Wilkinson D, Paterson KR, Jenkins L, Millais SB, Donoghue S. Evaluation of the safety and immunogenicity of synthetic Abeta42 (AN1792) in patients with AD. Neurology. 2005; 64:94–101. [PubMed: 15642910]
10. Salloway S, Gregg K, Black R, Grundman M, Sperling R. Cognitive and functional outcomes from a phase II trial of bapineuzumab in mild to moderate Alzheimer's disease. American Academy of Neurology Abs. 2009:S32.002.
11. Sperling, R.; Salloway, S.; Fox, N.; Barackos, J.; Morris, K.; Francis, G.; Black, R.; Grundman, M. Risk factors and clinical course associated with vasogenic edema in a phase II trial of

bapineuzumab.. Presentation at: 16th Congress of the European Federation of Neurological Societies; Stockholm, Sweden. 2009. http://www.stevenderoover.be/EFNS/Presentations/EFNS2012/WC220/.

12. Piazza F, Greenberg SM, Savoiardo M, Gardinetti M, Chiapparini L, Raicher I, Nitrini R, Sakaguchi H, Brioschi M, Billo G, et al. Anti-amyloid beta autoantibodies in cerebral amyloid angiopathy-related inflammation: Implications for Amyloid-Modifying Therapies. Ann Neurol. 2013
13. Ostrowitzki S, Deptula D, Thurfjell L, Barkhof F, Bohrmann B, Brooks DJ, Klunk WE, Ashford E, Yoo K, Xu ZX, et al. Mechanism of amyloid removal in patients with Alzheimer disease treated with gantenerumab. Arch Neurol. 2012; 69:198–207. [PubMed: 21987394]
14. Wilcock DM, Rojiani A, Rosenthal A, Subbarao S, Freeman MJ, Gordon MN, Morgan D. Passive immunotherapy against Abeta in aged APP-transgenic mice reverses cognitive deficits and depletes parenchymal amyloid deposits in spite of increased vascular amyloid and microhemorrhage. J Neuroinflammation. 2004; 1:24. [PubMed: 15588287]
15. Racke MM, Boone LI, Hepburn DL, Parsadainian M, Bryan MT, Ness DK, Piroozi KS, Jordan WH, Brown DD, Hoffman WP, et al. Exacerbation of cerebral amyloid angiopathy-associated microhemorrhage in amyloid precursor protein transgenic mice by immunotherapy is dependent on antibody recognition of deposited forms of amyloid beta. J Neurosci. 2005; 25:629–636. [PubMed: 15659599]
16. Callaway E. Alzheimer's drugs take a new tack. Nature. 2012; 489:13–14. [PubMed: 22962697]
17. Weksler ME, Relkin N, Turkenich R, LaRusse S, Zhou L, Szabo P. Patients with Alzheimer disease have lower levels of serum anti-amyloid peptide antibodies than healthy elderly individuals. Exp Gerontol. 2002; 37:943–948. [PubMed: 12086704]
18. Mruthinti S, Buccafusco JJ, Hill WD, Waller JL, Jackson TW, Zamrini EY, Schade RF. Autoimmunity in Alzheimer's disease: increased levels of circulating IgGs binding Abeta and RAGE peptides. Neurobiol Aging. 2004; 25:1023–1032. [PubMed: 15212827]
19. Kellner A, Matschke J, Bernreuther C, Moch H, Ferrer I, Glatzel M. Autoantibodies against beta-amyloid are common in Alzheimer's disease and help control plaque burden. Ann Neurol. 2009; 65:24–31. [PubMed: 19194878]
20. Britschgi M, Olin CE, Johns HT, Takeda-Uchimura Y, LeMieux MC, Rufibach K, Rajadas J, Zhang H, Tomooka B, Robinson WH, et al. Neuroprotective natural antibodies to assemblies of amyloidogenic peptides decrease with normal aging and advancing Alzheimer's disease. Proc Natl Acad Sci U S A. 2009; 106:12145–12150. [PubMed: 19581601]
21. Taguchi H, Planque S, Nishiyama Y, Szabo P, Weksler ME, Friedland RP, Paul S. Catalytic antibodies to amyloid beta peptide in defense against Alzheimer disease. Autoimmun Rev. 2008; 7:391–397. [PubMed: 18486927]
22. Taguchi H, Planque S, Sapparapu G, Boivin S, Hara M, Nishiyama Y, Paul S. Exceptional amyloid beta peptide hydrolyzing activity of nonphysiological immunoglobulin variable domain scaffolds. J Biol Chem. 2008; 283:36724–36733. [PubMed: 18974093]
23. Gao QS, Sun M, Rees AR, Paul S. Site-directed mutagenesis of proteolytic antibody light chain. J Mol Biol. 1995; 253:658–664. [PubMed: 7473741]
24. Ramsland PA, Terzyan SS, Cloud G, Bourne CR, Farrugia W, Tribbick G, Geysen HM, Moomaw CR, Slaughter CA, Edmundson AB. Crystal structure of a glycosylated Fab from an IgM cryoglobulin with properties of a natural proteolytic antibody. Biochem J. 2006; 395:473–481. [PubMed: 16422668]
25. Liu Y, Studzinski C, Beckett T, Guan H, Hersh MA, Murphy MP, Klein R, Hersh LB. Expression of neprilysin in skeletal muscle reduces amyloid burden in a transgenic mouse model of Alzheimer disease. Mol Ther. 2009; 17:1381–1386. [PubMed: 19471248]
26. Iwata N, Mizukami H, Shirotani K, Takaki Y, Muramatsu S, Lu B, Gerard NP, Gerard C, Ozawa K, Saido TC. Presynaptic localization of neprilysin contributes to efficient clearance of amyloid-beta peptide in mouse brain. J Neurosci. 2004; 24:991–998. [PubMed: 14749444]
27. Mukherjee A, Song E, Kihiko-Ehmann M, Goodman JP Jr. Pyrek JS, Estus S, Hersh LB. Insulysin hydrolyzes amyloid beta peptides to products that are neither neurotoxic nor deposit on amyloid plaques. J Neurosci. 2000; 20:8745–8749. [PubMed: 11102481]

28. Chesneau V, Vekrellis K, Rosner MR, Selkoe DJ. Purified recombinant insulin-degrading enzyme degrades amyloid beta-protein but does not promote its oligomerization. Biochem J. 2000; 351(Pt 2):509–516. [PubMed: 11023838]

29. Kou J, Kim HD, Pattanyak A, Song M, Lim J, Taguchi H, Paul S, Cirrito JR, Ponnazhagan S, Fukuchi K. Anti-Abeta single-chain antibody brain delivery via AAV reduces amyloid load but may increase cerebral hemorrhages in an Alzheimer mouse model. J Alzheimers Dis. 2011; 27:23–28. [PubMed: 21709371]

30. Niwa H, Yamamura K, Miyazaki J. Efficient selection for high-expression transfectants with a novel eukaryotic vector. Gene. 1991; 108:193–199. [PubMed: 1660837]

31. Grimm D, Kay MA, Kleinschmidt JA. Helper virus-free, optically controllable, and two-plasmid-based production of adeno-associated virus vectors of serotypes 1 to 6. Mol Ther. 2003; 7:839–850. [PubMed: 12788658]

32. Zolotukhin S, Potter M, Zolotukhin I, Sakai Y, Loiler S, Fraites TJ Jr. Chiodo VA, Phillipsberg T, Muzyczka N, Hauswirth WW, et al. Production and purification of serotype 1, 2, and 5 recombinant adeno-associated viral vectors. Methods. 2002; 28:158–167. [PubMed: 12413414]

33. Fukuchi KI, Tahara K, Kim HD, Maxwell JA, Lewis TL, Accavitti-Loper M, Kim H, Ponnazhagan S, Lalonde R. Anti-Aß single chain antibody delivery via adeno-associated virus for treatment of Alzheimer's disease. Neurobiol Dis. 2006; 23:502–511. [PubMed: 16766200]

34. Jankowsky JL, Fadale DJ, Anderson J, Xu GM, Gonzales V, Jenkins NA, Copeland NG, Lee MK, Younkin LH, Wagner SL, et al. Mutant presenilins specifically elevate the levels of the 42 residue beta-amyloid peptide in vivo: evidence for augmentation of a 42-specific gamma secretase. Hum Mol Genet. 2004; 13:159–170. [PubMed: 14645205]

35. DeMattos RB, Bales KR, Parsadanian M, O'Dell MA, Foss EM, Paul SM, Holtzman DM. Plaque-associated disruption of CSF and plasma amyloid-beta (Abeta) equilibrium in a mouse model of Alzheimer's disease. J Neurochem. 2002; 81:229–236. [PubMed: 12064470]

36. Minkeviciene R, Rheims S, Dobszay MB, Zilberter M, Hartikainen J, Fulop L, Penke B, Zilberter Y, Harkany T, Pitkanen A, et al. Amyloid beta-induced neuronal hyperexcitability triggers progressive epilepsy. J Neurosci. 2009; 29:3453–3462. [PubMed: 19295151]

37. Blennow K, Zetterberg H, Rinne JO, Salloway S, Wei J, Black R, Grundman M, Liu E. Effect of immunotherapy with bapineuzumab on cerebrospinal fluid biomarker levels in patients with mild to moderate Alzheimer disease. Arch Neurol. 2012; 69:1002–1010. [PubMed: 22473769]

38. Rinne JO, Brooks DJ, Rossor MN, Fox NC, Bullock R, Klunk WE, Mathis CA, Blennow K, Barakos J, Okello AA, et al. 11C-PiB PET assessment of change in fibrillar amyloid-beta load in patients with Alzheimer's disease treated with bapineuzumab: a phase 2, double-blind, placebo-controlled, ascending-dose study. Lancet Neurol. 2010; 9:363–372. [PubMed: 20189881]

39. Ferrer I, Boada RM, Sanchez Guerra ML, Rey MJ, Costa-Jussa F. Neuropathology and pathogenesis of encephalitis following amyloid-beta immunization in Alzheimer's disease. Brain Pathol. 2004; 14:11–20. [PubMed: 14997933]

40. Pfeifer M, Boncristiano S, Bondolfi L, Stalder A, Deller T, Staufenbiel M, Mathews PM, Jucker M. Cerebral hemorrhage after passive anti-Abeta immunotherapy. Science. 2002; 298:1379. [PubMed: 12434053]

41. Wilcock DM, Munireddy SK, Rosenthal A, Ugen KE, Gordon MN, Morgan D. Microglial activation facilitates Abeta plaque removal following intracranial anti-Abeta antibody administration. Neurobiol Dis. 2004; 15:11–20. [PubMed: 14751766]

42. Nicoll JA, Barton E, Boche D, Neal JW, Ferrer I, Thompson P, Vlachouli C, Wilkinson D, Bayer A, Games D, et al. Abeta species removal after abeta42 immunization. J Neuropathol Exp Neurol. 2006; 65:1040–1048. [PubMed: 17086100]

43. Moreth J, Mavoungou C, Schindowski K. Passive anti-amyloid immunotherapy in Alzheimer's disease: What are the most promising targets? Immun Ageing. 2013; 10:18. [PubMed: 23663286]

44. Tayeb HO, Murray ED, Price BH, Tarazi FI. Bapineuzumab and solanezumab for Alzheimer's disease: is the ‘amyloid cascade hypothesis’ still alive? Expert Opin Biol Ther. 2013; 13:1075–1084. [PubMed: 23574434]

45. Adolfsson O, Pihlgren M, Toni N, Varisco Y, Buccarello AL, Antoniello K, Lohmann S, Piorkowska K, Gafner V, Atwal JK, et al. An effector-reduced anti-beta-amyloid (Abeta) antibody

with unique abeta binding properties promotes neuroprotection and glial engulfment of Abeta. J Neurosci. 2012; 32:9677–9689. [PubMed: 22787053]

46. Fukuchi KI, Accavitti-Loper M, Kim HD, Tahara K, Cao Y, Lewis TL, Caughey RC, Kim H, Lalonde R. Amelioration of amyloid load by anti-A[beta] single-chain antibody in Alzheimer mouse model. Biochem Biophys Res Commun. 2006; 344:79–86. [PubMed: 16630540]
47. Kou J, Song M, Pattanayak A, Lim J, Yang J, Cao D, Li L, Fukuchi K. Combined treatment of Aß immunization with statin in a mouse model of Alzheimer's disease. J Neuroimmunol. 2012; 244:70–83. [PubMed: 22326143]
48. Cearley CN, Wolfe JH. Transduction characteristics of adeno-associated virus vectors expressing cap serotypes 7, 8, 9, and Rh10 in the mouse brain. Mol Ther. 2006; 13:528–537. [PubMed: 16413228]
49. Cearley CN, Wolfe JH. A single injection of an adeno-associated virus vector into nuclei with divergent connections results in widespread vector distribution in the brain and global correction of a neurogenetic disease. J Neurosci. 2007; 27:9928–9940. [PubMed: 17855607]
50. Van der Perren A, Toelen J, Carlon M, Van Den Haute C, Coun F, Heeman B, Reumers V, Vandenberghe LH, Wilson JM, Debyser Z, et al. stable transduction of dopaminergic neurons in rat substantia nigra by rAAV 2/1, 2/2, 2/5, 2/6.2, 2/7, 2/8 and 2/9. Efficient and. Gene Ther. 2011; 18:517–527.
51. Samaranch L, Salegio EA, San SW, Kells AP, Bringas JR, Forsayeth J, Bankiewicz KS. Strong cortical and spinal cord transduction after AAV7 and AAV9 delivery into the cerebrospinal fluid of nonhuman primates. Hum Gene Ther. 2013; 24:526–532. [PubMed: 23517473]
52. Harry GJ. Microglia during development and aging. Pharmacol Ther. 2013; 139:313–326. [PubMed: 23644076]
53. Jimenez S, Baglietto-Vargas D, Caballero C, Moreno-Gonzalez I, Torres M, Sanchez-Varo R, Ruano D, Vizuete M, Gutierrez A, Vitorica J. Inflammatory response in the hippocampus of PS1M146L/APP751SL mouse model of Alzheimer's disease: age-dependent switch in the microglial phenotype from alternative to classic. J Neurosci. 2008; 28:11650–11661. [PubMed: 18987201]
54. Bard F, Cannon C, Barbour R, Burke RL, Games D, Grajeda H, Guido T, Hu K, Huang J, Johnson-Wood K, et al. Peripherally administered antibodies against amyloid beta-peptide enter the central nervous system and reduce pathology in a mouse model of Alzheimer disease. Nat Med. 2000; 6:916–919. [PubMed: 10932230]
55. Banks WA, Terrell B, Farr SA, Robinson SM, Nonaka N, Morley JE. Passage of amyloid beta protein antibody across the blood-brain barrier in a mouse model of Alzheimer's disease. Peptides. 2002; 23:2223–2226. [PubMed: 12535702]
56. Iwata N, Sekiguchi M, Hattori Y, Takahashi A, Asai M, Ji B, Higuchi M, Staufenbiel M, Muramatsu S, Saido TC. Global brain delivery of neprilysin gene by intravascular administration of AAV vector in mice. Sci Rep. 2013; 3:1472. [PubMed: 23503602]
57. Carty N, Nash KR, Brownlow M, Cruite D, Wilcock D, Selenica ML, Lee DC, Gordon MN, Morgan D. Intracranial injection of AAV expressing NEP but not IDE reduces amyloid pathology in APP+PS1 transgenic mice. PLoS ONE. 2013; 8:e59626. [PubMed: 23555730]
58. Tucker HM, Kihiko-Ehmann M, Estus S. Urokinase-type plasminogen activator inhibits amyloid-beta neurotoxicity and fibrillogenesis via plasminogen. J Neurosci Res. 2002; 70:249–255. [PubMed: 12271474]
59. Fu H, Muenzer J, Samulski RJ, Breese G, Sifford J, Zeng X, McCarty DM. Self-complementary adeno-associated virus serotype 2 vector: global distribution and broad dispersion of AAV-mediated transgene expression in mouse brain. Mol Ther. 2003; 8:911–917. [PubMed: 14664793]
60. Foust KD, Nurre E, Montgomery CL, Hernandez A, Chan CM, Kaspar BK. Intravascular AAV9 preferentially targets neonatal neurons and adult astrocytes. Nat Biotechnol. 2009; 27:59–65. [PubMed: 19098898]
61. Duque S, Joussemet B, Riviere C, Marais T, Dubreil L, Douar AM, Fyfe J, Moullier P, Colle MA, Barkats M. Intravenous administration of self-complementary AAV9 enables transgene delivery to adult motor neurons. Mol Ther. 2009; 17:1187–1196. [PubMed: 19367261]

62. Fu H, Dirosario J, Killedar S, Zaraspe K, McCarty DM. Correction of neurological disease of mucopolysaccharidosis IIIB in adult mice by rAAV9 trans-blood-brain barrier gene delivery. Mol Ther. 2011; 19:1025–1033. [PubMed: 21386820]

63. Spampanato C, De LE, Dama P, Gargiulo A, Fraldi A, Sorrentino NC, Russo F, Nusco E, Auricchio A, Surace EM, et al. Efficacy of a combined intracerebral and systemic gene delivery approach for the treatment of a severe lysosomal storage disorder. Mol Ther. 2011; 19:860–869. [PubMed: 21326216]

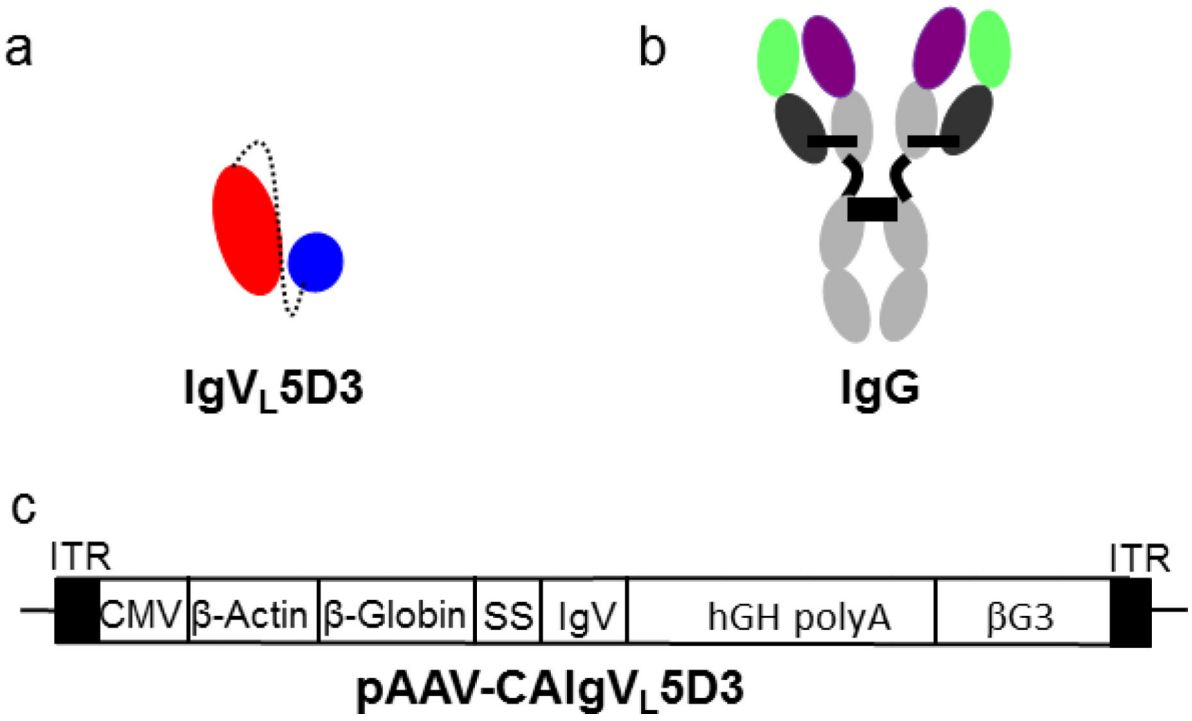

Fig 1. Schematic representation of IgV$_L$5D3 and its expression vector, pAAV-CAIgV$_L$5D3

IgV$_L$ 5D3 is a single domain VL (red) with *a tag* at the C terminus, corresponding to the peptide Linker (dashed line), a short peptide region in place of the VH domain and the His6/c-*myc* tag tag (blue) (a). Typical IgG structure is shown as a reference (b). pAAV-CAIgV$_L$5D3 (c). ITR: inverted terminal repeats; CMV: cytomegalovirus enhancer; β-actin: β-actin promoter; β-globin: β-globin intron; SS: signal sequence; IgV: cDNA for IgV; hGH polyA: human growth hormone polyadenylation signal; βG3: rabbit β-globin 3' non-cording sequence.

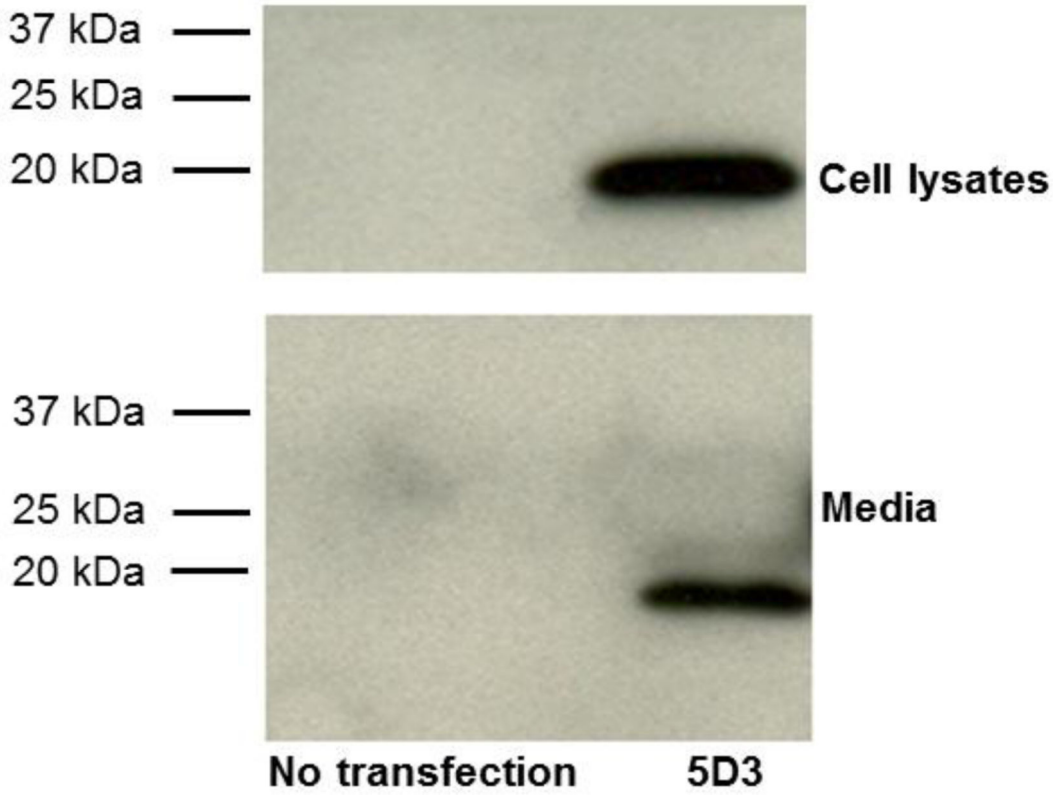

Fig 2. Expression and secretion of IgV_L5D3 in cultured HEK293 cells

HEK293 cells were transfected with pAAV-CAIgV_L5D3. Three days after transfection, the media were collected and cells were harvested. Forty micrograms protein/lane of cell lysate was loaded on 4 –15 % Tris-HClpolyacrylamide gel. For media, 10 μl of medium from each sample was loaded on the same gel. Samples from nontransfected HEK293 cells were used as negative controls. After electrophoresis and electroblotting to a PVDF membrane, IgVs were visualized by anti-c-Myc antibody.

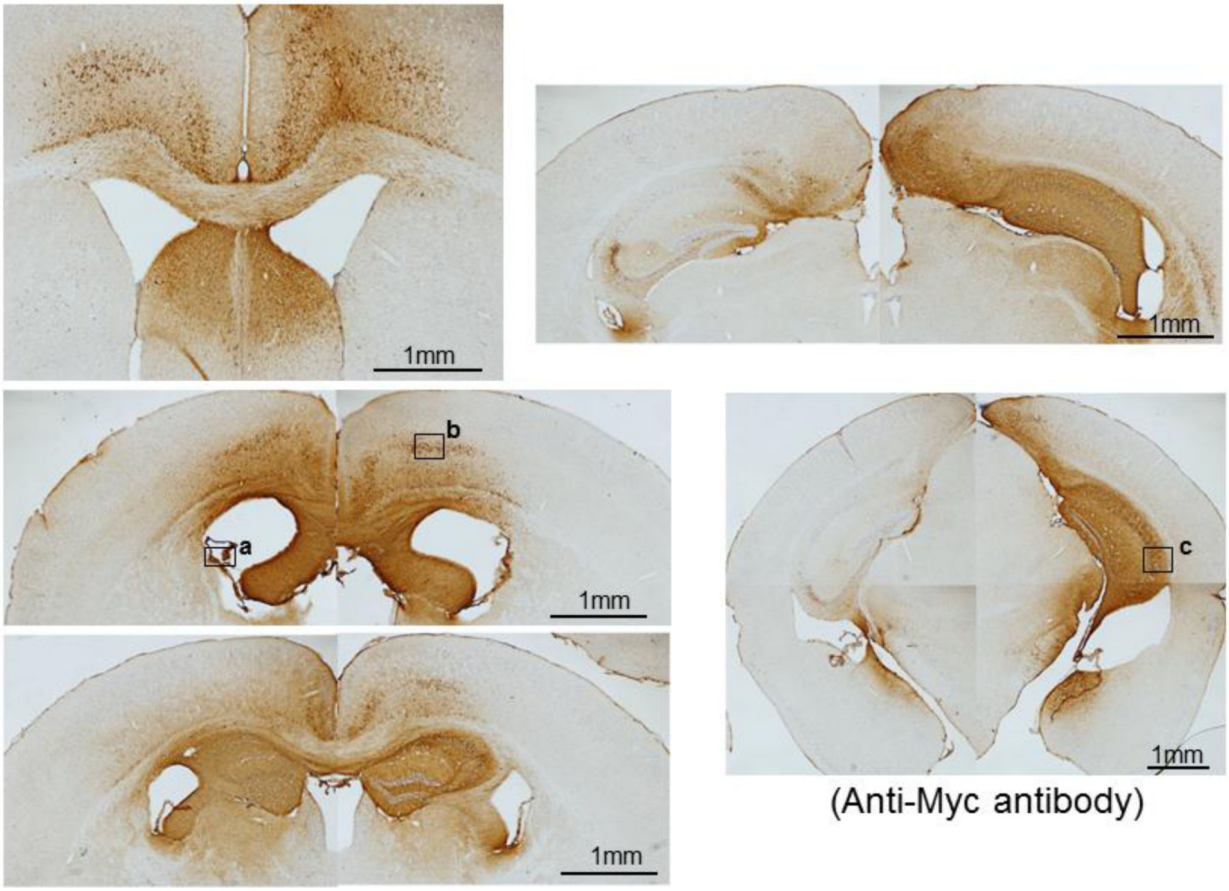

Fig 3. IgV_L5D3 is predominantly expressed in the right brain hemisphere

rAAV9-IgV_L5D3 was injected into the right lateral ventricle of TgAPPswe/PS1dE9 mice and, 8 (prophylaxis) and 5 (therapy) months after the injection, IgV_L5D3 expression in the brain was visualized by immunohistochemistry using anti-c-Myc antibody. Brain sections from a representative mouse are shown. Scale bars, 1 mm. High magnification pictures of the areas indicated by the squares (a through c) are found in Supplemental Figure 1.

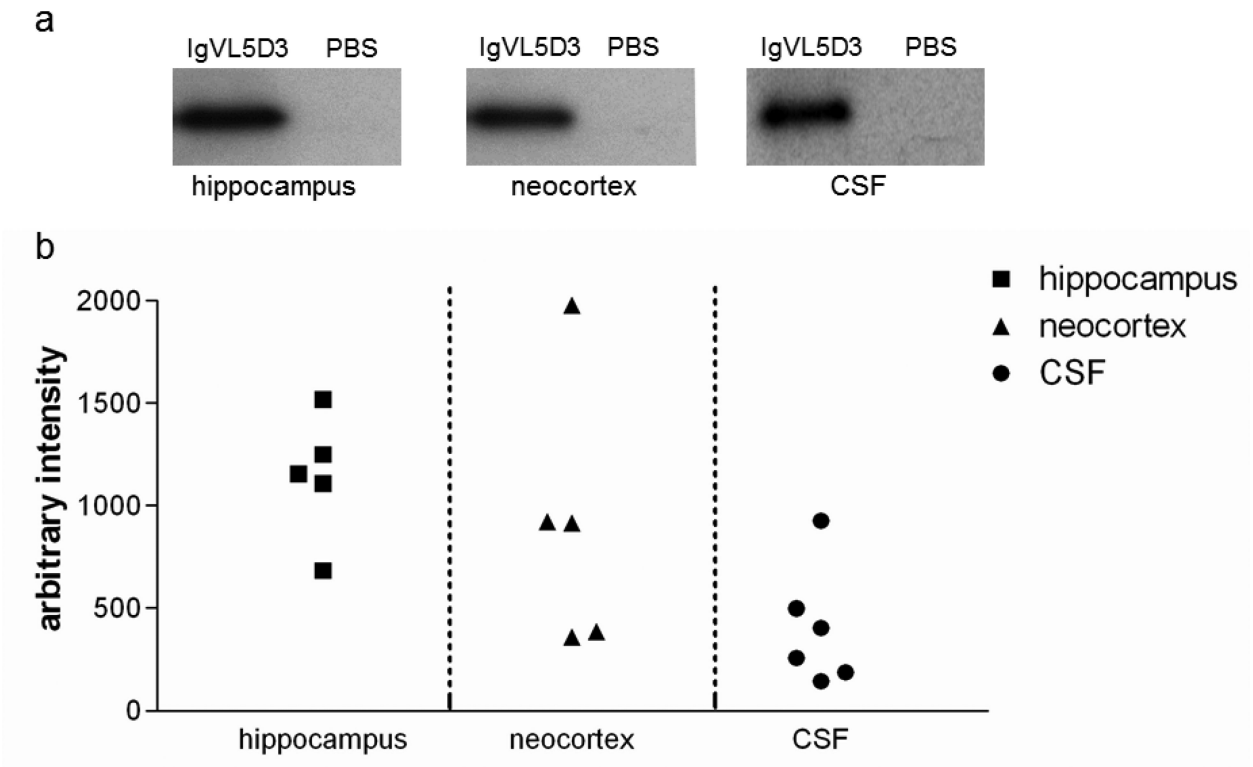

Fig 4. Levels of IgV_L5D3 expression are high in the left hippocampus but vary in the neocortex

Five months after rAAV9-IgV_L5D3 injection, hippocampal and neocortex homogenates and CSF were prepared and subjected to 10– 20 % SDS PAGE followed by immunoblotting using anti-c-Myc antibody to determine expression levels of IgV_L5D3. A mouse subjected to PBS injection was used as a negative control. Sixty μg of total protein for the homogenates and 10 μl of CSF were loaded on each lane. IgV_L5D3 bands visualized by anti-c-Myc antibody are shown as a representative sample for hippocampus, neocortex, and CSF (a). The optical density of an IgV_L5D3 band from each sample is plotted after normalization with the GAPDH band except CSF (b).

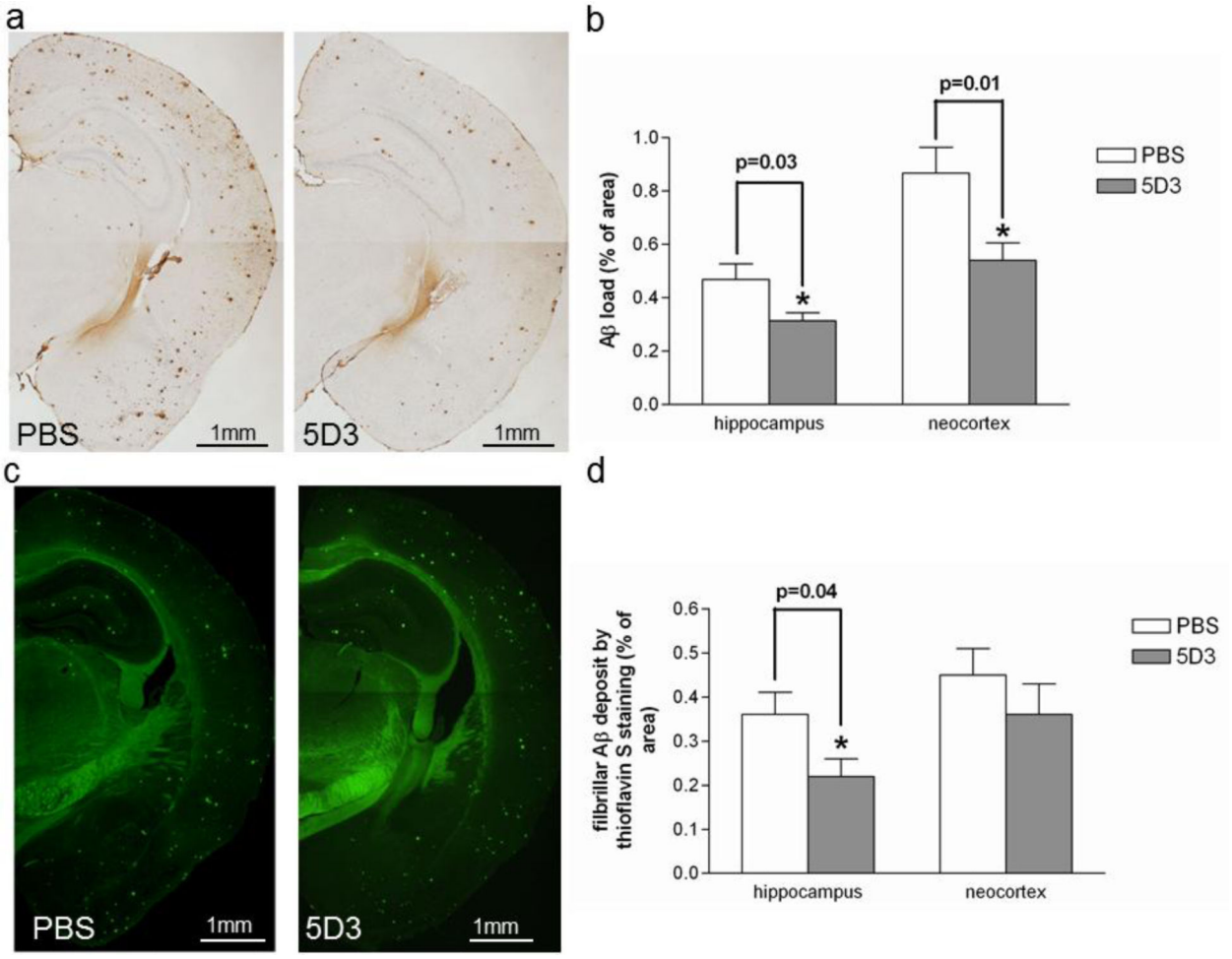

Fig 5. Prophylactic rAAV9-IgV$_L$5D3 injection decreases Aβ load in the right hippocampus

Eight months after rAAV9 or PBS injection, TgAPPswe/PS1dE9 mice were terminated and Aβ deposits in the brain were visualized and quantified by morphometric analysis. Aβ deposits are visualized by 6E10 antibody (a, b) and thioglavine S (c, d). The percentages of immunoreactive or fluorescent areas for 6E10 (b) and thioflavin S (d), respectively, are shown as bar graphs. The values shown are the mean ± SEM. PBS: PBS-injected mouse, 5D3: rAAV9-IgV$_L$5D3-injected mouse. Scale bars, 1 mm.

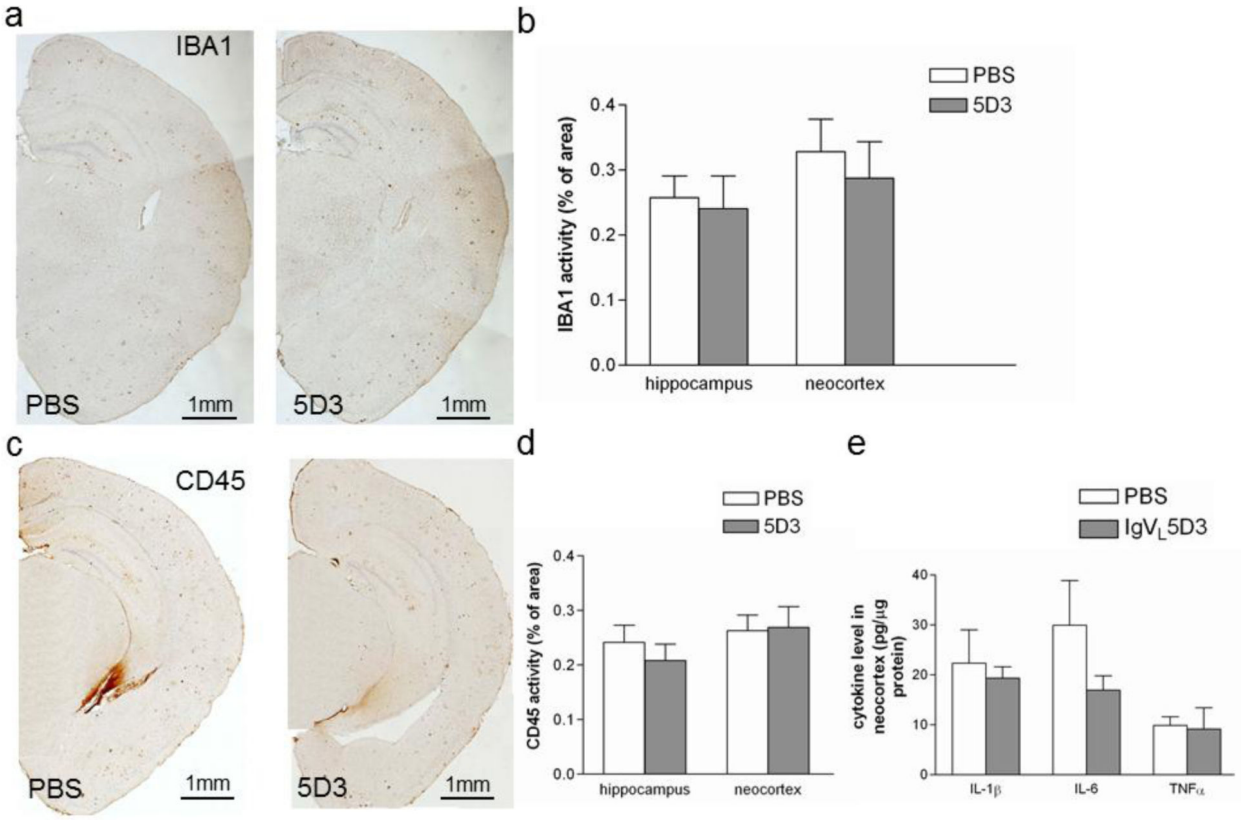

Fig 6. Prophylactic rAAV9-IgV$_L$5D3 injection does not increase expression levels of microglia activation markers and proinflammatory cytokines

Eight months after rAAV9 or PBS injection, activated microglia and/or monocytes in the right hippocampus and neocortex were visualized by immunohistochemistry using anti-Iba1 (a) and anti-CD45 (b) antibody, and quantified by morphometric analysis (c and d, respectively). The percentages of Iba1- and CD45-immunoreactive areas are shown as bar graphs (b and c, respectively). Pro-inflammatory cytokine levels in the left neocortex homogenates were determined by ELISA (e). The values shown are the mean ± SEM. Scale bars, 1 mm.

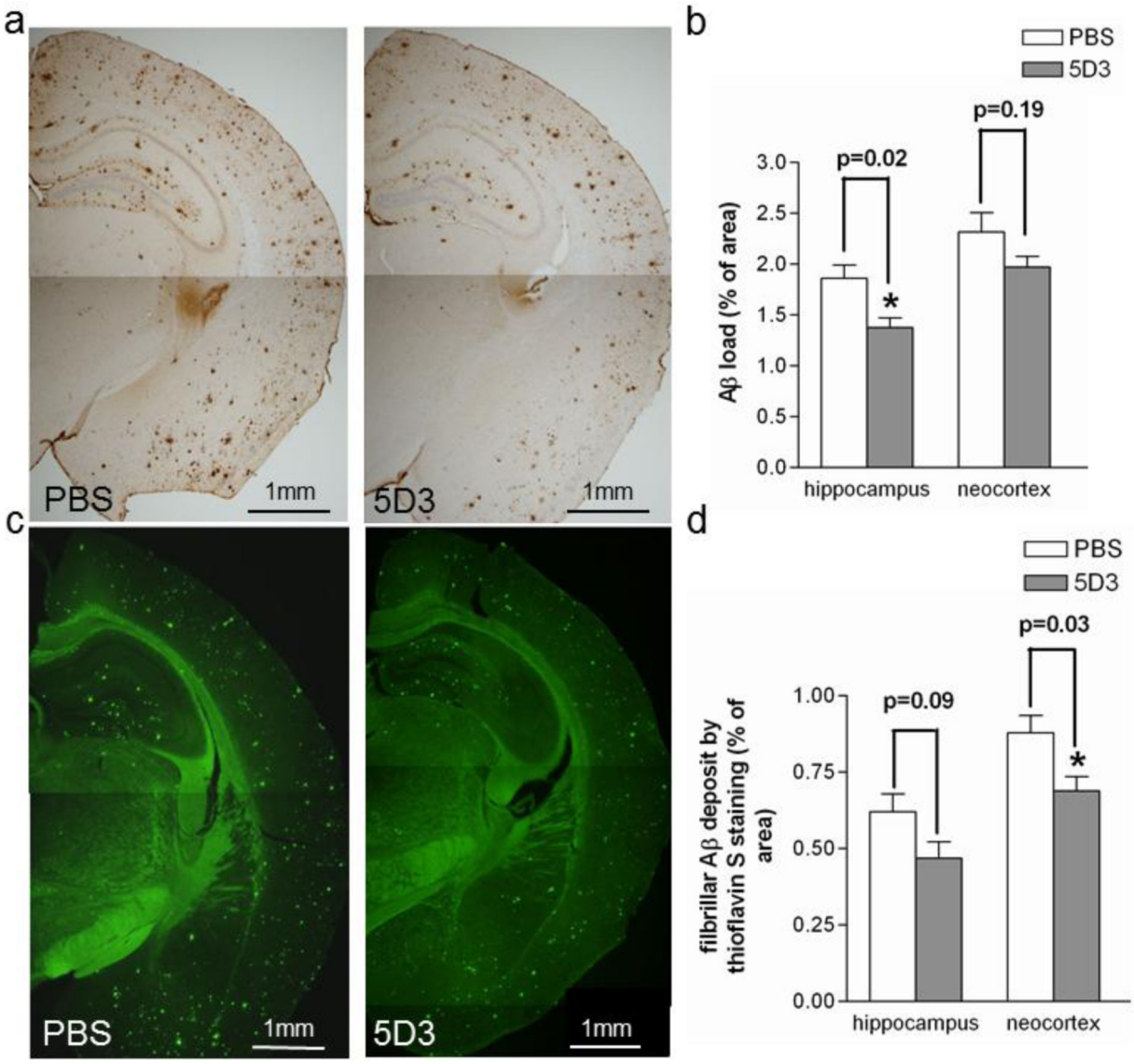

Fig 7. Therapeutic rAAV9-IgV$_L$5D3 injection decreases Aβ-immunoreactive deposits in the right hippocampus and fibrillar Aβ-deposits in the right neocortex

Five months after rAAV9-IgV$_L$5D3 or PBS injection, TgAPPswe/PS1dE9 mice were terminated and Aβ deposits in the brain were visualized and quantified by morphometric analysis. Aβ deposits are visualized by 6E10 antibody (a, b) and thioflavin S (c, d). The percentages of immunoreactive or fluorescent areas for 6E10 (b) and thioflavin S (d), respectively, are shown as bar graphs. The values shown are the mean ± SEM. PBS: PBS-injected mouse, 5D3: rAAV9-IgV$_L$5D3-injected mouse. Scale bars, 1 mm.

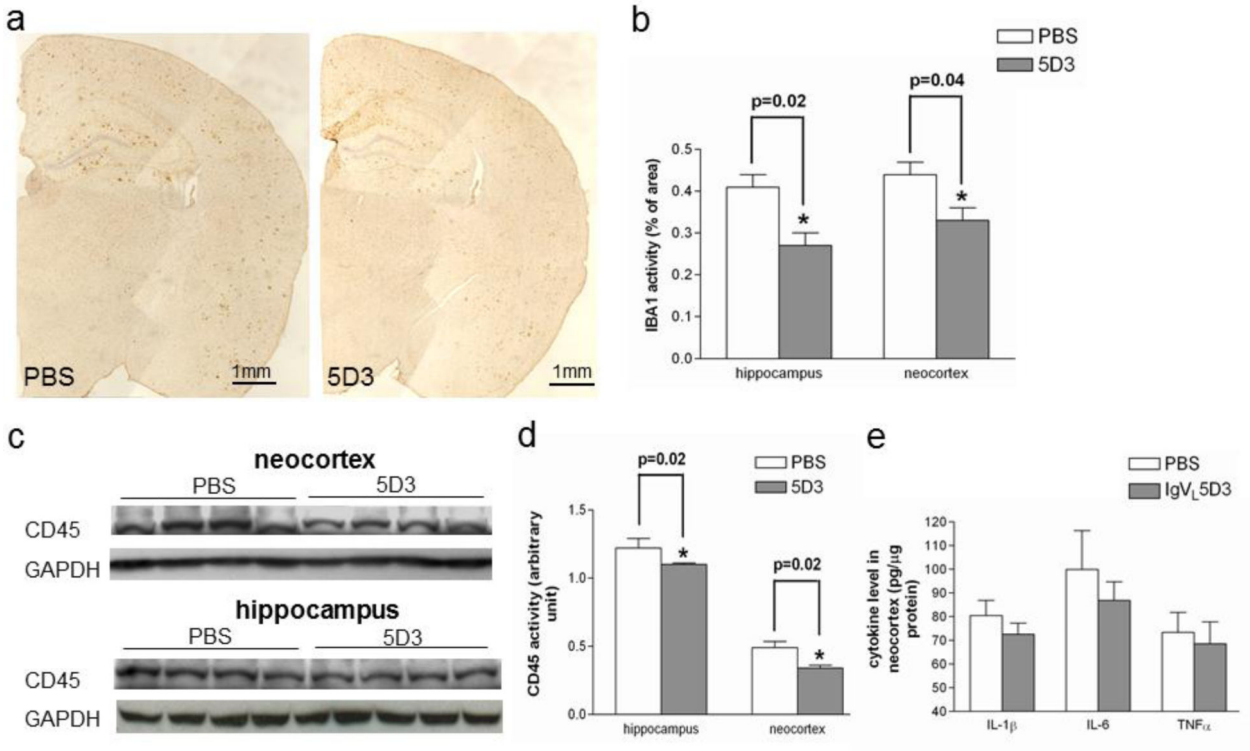

Fig 8. Therapeutic rAAV9-IgV$_L$5D3 injection decreases microglia/monocyte activation

Five months after rAAV9 or PBS injection, activated microglia and/or monocytes in the right hippocampus and neocortex were visualized by immunohistochemistry using anti-Iba1 antibody (a) and quantified by morphometric analysis. The percentages of Iba1-immunoreactive areas are shown as bar graphs (b). Homogenates of the left hippocampi and neocortices were subjected to SDS-PAGE followed by immunoblotting using anti-CD45 antibody (c). The bar graph represents the optical density ratio to that of the GAPDH band on the same lane (d). Pro-inflammatory cytokine levels in the left neocortex homogenates were determined by ELISA (e). The values shown are the mean ± SEM. Scale bars, 1 mm.

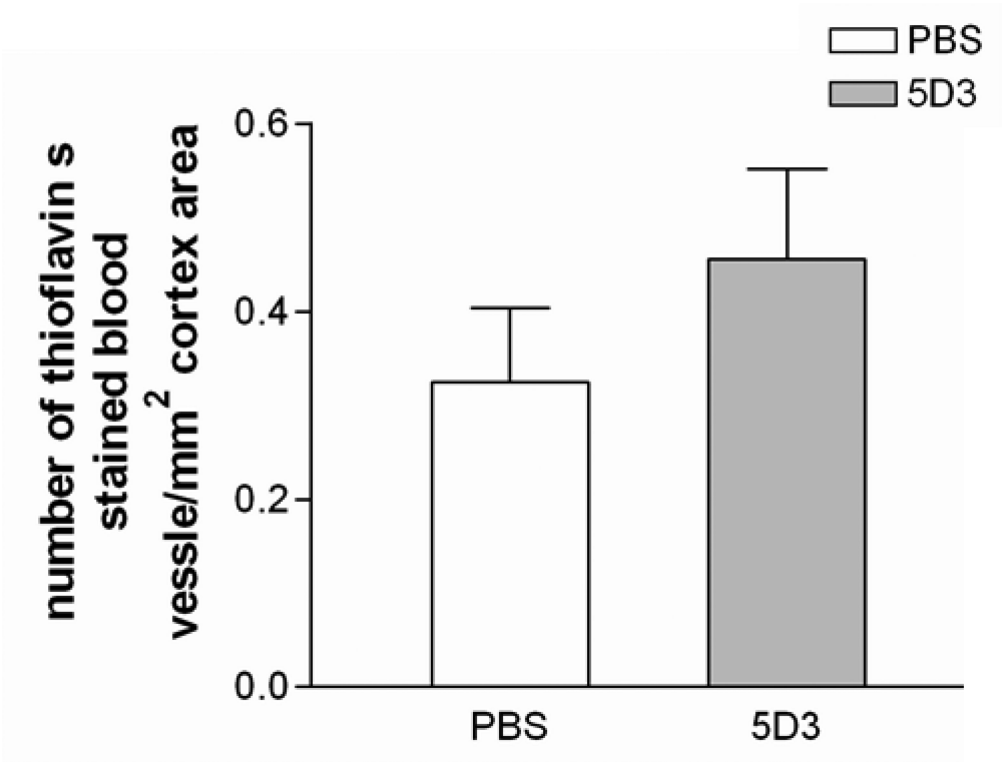

Fig 9. Therapeutic rAAV9-IgV$_L$5D3 injection does not increase cerebral amyloid angiopathy

Five months after rAAV9 or PBS injection, cerebral amyloid angiopathy (CAA) in the right hippocampus and neocortex were visualized by thioflavin S fluorescence and blood vessels positive for thioflavin S fluorescence were enumerated. The numbers of blood vessels positive for thioflavin S fluorescence per square millimeter are shown (mean ± SEM).

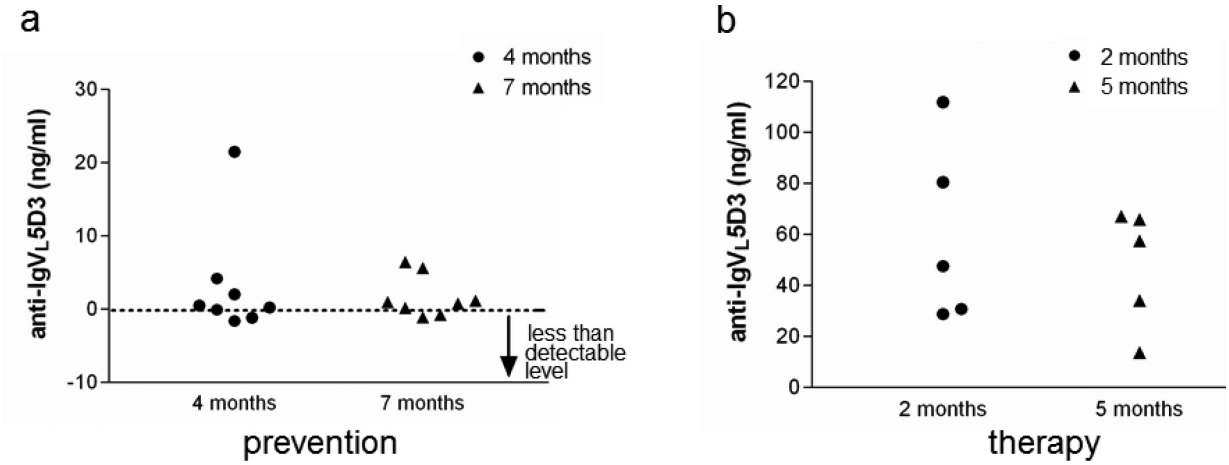

Fig 10. Induction of anti-IgV$_L$5D3 antibody by rAAV9-IgV$_L$5D3 injection is negligible

Four and seven months after prophylactic rAAV9-IgV$_L$5D3 injection, sera were collected and anti- IgV$_L$5D3 IgG titers were determined by ELISA. Each anti-IgV$_L$5D3titer from each TgAPPswe/PS1dE9 mouse subjected to rAAV9-IgV$_L$5D3 injection is shown (a). Two and five months after therapeutic prophylactic rAAV9-IgV$_L$5D3 injection, serum from each mouse was similarly analyzed and is shown (b).

Table 1

The numbers of mice used for the prophylactic study. Mice were subjected to rAAV9 or PBS injections at 2 months of age and terminated at 10 months

	Number of mice subjected to AAV injection		Number of mice that survived and were examined		Number of mice that died during treatment	
	PBS	**IgV_L5D3**	**PBS**	**IgV_L5D3**	**PBS**	**IgV_L5D3**
TgAPPswe/PS1dE male	9	9	6	5	3	4
TgAPPswe/PS1dE female	8	9	5	5	3	4
Non-Tg male	7	7	6	6	1	1
Non-Tg female	8	7	6	7	2	0

Table 2

The numbers of mice used for the therapeutic study. Mice were subjected to rAAV9 or PBS injections at 10 months of age and terminated at 15 months

	Number of mice subjected to AAV injection		Number of mice that survived and were examined		Number of mice that died during treatment	
	PBS	**IgV$_L$5D3**	**PBS**	**IgV$_L$5D3**	**PBS**	**IgV$_L$5D3**
TgAPPswe/PS1dE male	5	5	5	4	0	1
TgAPPswe/PS1dE female	3	2	3	1	0	1
Non-Tg male	5	7	4	7	1	0
Non-Tg female	3	4	3	3	0	1